Orbit feedback system for maintaining an optimum beam collision

Y. Funakoshi, M. Masuzawa, K. Oide, J. Flanagan, M. Tawada, T. Ieiri, M. Tejima, M. Tobiyama, K. Ohmi, and H. Koiso

High Energy Accelerator Research Organization (KEK), 1-1 Oho, Ibaraki 305-0801, Japan

(Received 13 September 2007; published 25 October 2007)

An orbit feedback system around the interaction point (IP) has been developed and successfully employed at KEKB for more than 6 years. The purpose of the system is to maintain an optimum geometrical relationship of orbits of two beams at the IP and to prevent a luminosity degradation due to orbit drifts. The feedback system is based on orbit measurements around the IP rather than a direct measurement of the luminosity. Owing to the system, the luminosity degradation due to the orbit drifts is suppressed to around or less than 1%.

DOI: 10.1103/PhysRevSTAB.10.101001 PACS numbers: 29.20.Dh, 29.27.Bd

I. INTRODUCTION

The KEKB B-factory is a second generation electron-positron collider. It has two significant features of a very high luminosity and an energy asymmetry. These features come from requirements of *B* meson physics which studies very rare processes and aims at studying the *CP* violating effects in the *B* meson system. The design peak luminosity is $1 \times 10^{34}/\mathrm{cm}^2/\mathrm{sec}$. The KEKB luminosity surpassed this design value in May of 2003. The present record is $1.71 \times 10^{34}/\mathrm{cm}^2/\mathrm{sec}$ as of July 1, 2007. Beam energies are 3.5 GeV for the low-energy ring (LER, $e+$) and 8 GeV for the high-energy ring (HER, $e-$). The requirement of energy asymmetry inevitably leads us to the scheme of a double-ring collider. From the standpoint of machine design, this double-ring scheme enables a high current-multibunch approach like synchrotron light sources, which is vital to reach a higher luminosity. In addition to these features, KEKB adopted a challenging scheme of a horizontal crossing angle of ± 11 mrad. A motivation of the crossing angle is to simplify the IR (interaction region) design and to suppress effects of parasitic crossings [1].

A. Need for the system

In double-ring colliders such as KEKB, we have to solve some special problems which we never encountered in conventional single-ring colliders. One such critical problem is how to maintain optimum beam collision conditions. For this purpose, we have developed a special system which manipulates beam orbits around the IP. Without this kind of system, the two beams do not meet each other properly at the IP and serious degradation of the luminosity results, since two beams circulate in different rings and the beam orbits of the two beams may possibly drift independently due to different drifting sources. The system controls two parameters related to the beam orbits; i.e. the vertical beam offset of the two beams at the IP and the vertical crossing angle. We do not care about the horizontal crossing angle in usual machine operations. This is because the machine performance does not depend very much on the horizontal crossing angle. We employ a relatively large horizontal crossing angle of ± 11 mrad and an additional horizontal crossing angle from drifts of the orbits is usually negligibly small compared with this intentionally introduced crossing angle. As for the horizontal offset, at present we do not apply the orbit feedback system whose algorithm we describe in this paper.

B. Principle of the system

The purpose of the system is to maintain optimum collision conditions. When we designed the system, we considered two possible methods for this purpose. One is a method based on measurements of the luminosity (luminosity-driven system). The other is based on measurements of the beam orbits around the IP. The former is straightforward in the sense that the luminosity is the ultimate goal of the factory machines. However, when the luminosity degradation due to the orbit drift is observed, we cannot know in which direction we should change the orbits for recovery of the luminosity. Therefore, we have to change the orbits continuously in some manner so as to maximize the luminosity with this method. This intentional change of the orbits for searching the optimum collision conditions may bring some loss in the luminosity. On the other hand, with the latter method we can know in which direction we should change the orbits when an orbit drift is detected. If accuracy of the orbit measurements is enough, we may sustain the optimum collision conditions with almost no loss of luminosity. We have adopted this method mainly for this reason. Another reason for our choice is that our fast luminosity monitor has rather poor performance, in the sense that the luminosity monitor has relatively narrow acceptance and small changes of the orbit around the IP affect its measurement. Possible problems with this method are the accuracy of the orbit measurements and the long-term stability of the orbit measurement system. For example,

 © 2007 The American Physical Society

if mechanical positions of beam position monitors (BPMs) are changed for some reason, that may affect system performance. These issues are discussed in detail in this paper. To detect an orbit offset at the IP, which is a relative position difference of the two beams at the IP, we adopted a beam-beam deflection technique (deflection-driven system). This technique is based on the idea that the orbit offset at the IP brings dipole kicks due to the beam-beam force proportional to the offset in the linear region. By measuring orbit changes due to these dipole kicks, we can estimate the offset. As is shown in this paper, the beam-beam deflection method is particularly important for detection of the vertical offset, since a vertical offset which brings a significant luminosity degradation appears not to be easy to detect by measuring orbit drifts. This technique was first applied at the SLAC linear collider (SLC) [2,3]. Its effectiveness was proved also in a ring collider [4,5]. As for the vertical crossing angle of the two beams, we estimate the value simply by measuring orbits of the two beams around the IP.

At KEKB, we have been successfully employing an orbit feedback system based on the principle described above for more than 6 years. In the previous papers, we gave minimum descriptions of the system [6,7]. In this paper, we give more detailed descriptions of the system and experience in actual beam operations.

In PEP-II which is another B-factory in the world, a luminosity-driven feedback system has been successfully utilized since the very beginning of its history [8,9]. A comparison between the deflection-driven and the luminosity-driven feedback system is discussed in Sec. V.

II. DESCRIPTION OF FEEDBACK SYSTEM

In this section, we give a detailed description of the feedback system. First, we describe a configuration of the hardware components. Then, we explain the feedback parameters and the feedback algorithm with which the feedback system works.

A. Layout of the feedback system

The system is composed of 6 BPMs, 12 steering magnets, power supplies for the magnets, signal processing devices for the BPMs, and a control system.

1. BPM system

Locations of the 6 BPMs are shown schematically in Fig. 1. As shown in the figure, 2 of 6 BPMs (E and F) are special BPMs called "OctoPos." The OctoPos BPMs are located closer to the IP than the other BPMs. They have 8 electrodes and can measure orbits of the two beams simultaneously. On the other hand, the other 4 BPMs (A, B, C, and D) are conventional ones for measuring beam orbits of one beam. To ensure sufficient accuracy of the measurements, the orbit measurements using these BPMs are done

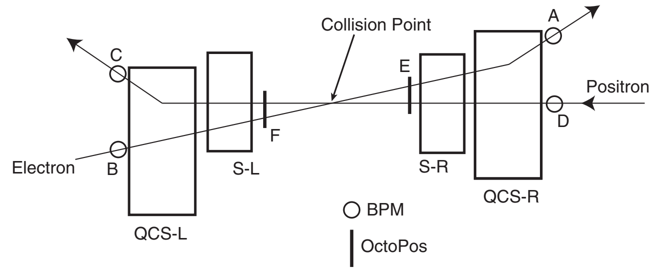

FIG. 1. Schematic view of BPM configuration.

in an averaging mode, so we cannot know turn-by-turn positions of the beams but rather the averaged orbits. Measurements of beam orbits are the basis of our feedback system and impose a fundamental restriction on system performance. Typical position resolution of the orbit measurements is around 2 μm. As is shown below, this resolution is good enough for our purpose. A typical repetition time of the measurement by using the usual BPMs including the QCS BPMs (A, B, C, and D) is 4 seconds. Here, QCS represents a pair of superconducting quadrupole magnets nearest to the IP. On the other hand, the OctoPos BPMs have their own read-out system and the position information can be updated as quickly as every second. The repetition time of the orbit feedback is mainly determined by this orbit measurement time.

As is shown below, in principle, a set of 4 QCS BPMs (A, B, C, and D) or another set of 2 OctoPos BPMs (E and F) gives sufficient information to the feedback system. In actual beam operation, we usually use the set of 4 regular BPMs, since the beam current dependence in the orbit measurements is larger with the set of OctoPos BPMs than with the regular BPMs. This beam current dependence of the OctoPos system makes the feedback operation difficult in some situations [10] as is discussed below. On the other hand, the regular BPM system may possibly have a problem if kicks by the QCSR (one of the QCS magnets on the right side of the IP) or QCSL (the other QCS magnets on the left side of the IP) change from time to time, since these kicks interfere with the translation from the position measurements at the BPMs to the beam-beam kick at the IP. These changes can be induced by mechanical position shifts of the QCS magnets or by use of the steering magnets incorporated in these same QCS magnets. In the actual beam operations, however, these changes are relatively small, provided that we do not use the steering magnets of the QCS. Technical details on the OctoPos and the usual BPM systems are written in other papers [10,11].

2. Control system

Almost all accelerator components at KEKB are controlled by the system based on EPICS [12]. In this system, a control computer called "IOC (input output controller)" is located at each local control room. Each IOC controls

VERSA Module European (VME) modules in a sub-rack in which the IOC itself is contained. The VME modules control directly or indirectly the accelerator components. In the case of BPMs used in KEKB, raw signals from the BPMs are processed with front end circuits in a VME bus extensions for instrumentation (VXI) mainframe. The processed signals are sent to a VME module through multisystem extension interface bus (MXI) modules [11]. The processed signals from BPMs are recorded in the IOCs as EPICS database records. The IOCs are connected with each other through a network. A cluster of workstations based on UNIX are also connected to the network. In our feedback system, the feedback routine works in one of the workstations. For this purpose, an application program has been developed. This application is written in SAD script [13] developed at KEK. A man-machine interface is also realized in this application. By using this interface, machine operators can control the feedback routine. The application program can access the hardware by referencing the EPICS records.

3. Steering magnets

For the control of beam orbits, we employ 12 steering magnets on the left and right sides of the IP in the HER, of which 4 are horizontal steering magnets and the other 8 are used in the vertical direction. These steering magnets are dedicated to the orbit feedback. We do not use steering magnets in the LER for the present purpose, since the IR of the LER is crowded with magnets for the local correction [1] and no room is left for installation of additional steering magnets. Of the 8 vertical steering magnets, 4 are located in the straight section in the IR and another 4 are placed in the arc section near the IR. The orbit feedback handles the vertical offset at the IP and the vertical crossing angle. These are handled by making local bump orbits around the IP. If our purpose is only to make a closed orbit, four vertical steering magnets are enough. However, an asymmetric bump at the IP, which handles the vertical crossing angle, creates a huge vertical dispersion which cannot be suppressed within the straight section near the IP. To suppress the vertical dispersion, another four vertical steering magnets in an arc section are used. By making vertical bumps at the sextupole magnets where a large horizontal dispersion exists, the vertical dispersion can be effectively suppressed. In KEKB, a noninterleaved sextupole magnet scheme is adopted [1]. An symmetric vertical orbit bump at a pair of the sextupole magnets makes a large vertical dispersion around the ring. On the other hand, the x-y coupling components induced by the vertical orbit at the sextupole magnets are localized between the paired sextupole magnets. By combining the asymmetric bump around the IP and the two asymmetric bumps in arc sections on both sides of the IP, the vertical dispersion created around the IP is corrected within the bump section.

Another thing that we have to consider is the mutual interference of the horizontal and the vertical orbit bumps at the IP. Since some of the steering magnets for making the bumps are located at the positions where the x-y coupling does not vanish, the horizontal bumps make some vertical offset or angle at the IP and vice versa. To avoid these interferences, we always employ all the 12 steering magnets when we make any kind of bump.

The power supplies of the steering magnets are controlled by using a DAC module based on the CAMAC system. The CAMAC system is connected to a VME interface module and then is controlled by an IOC. The currents of the power supplies are monitored by a CAMAC analog-to-digital converter. The feedback application can set to or read from the power supplies by accessing the EPICS database records. We have developed a special type of steering magnet for the feedback. To avoid damage of a physics detector component (vertex detector), the critical energy of the synchrotron radiation emitted from the magnets near the IP is limited to be less than 1 keV. Considering this limitation, we built relatively weak steering magnets, and so the dynamic range of the orbit control is relatively narrow. The system can change only $\pm 180\ \mu$m and ± 0.3 mrad at the IP in the vertical direction. The DAC which controls the steering magnets has ± 2048 steps.

B. Feedback parameters

The beam position for the feedback is monitored by the BPMs on the superconducting quadrupole magnet (QCS). With the QCS BPMs in the HER located at positions A and B and the LER BPMs at C and D, the vertical beam positions at A and B are written as

$$y_e^A = m_{33}^A y_e^* + m_{34}^A y_e^{\prime *a} \tag{1}$$

$$y_e^B = m_{33}^B y_e^* + m_{34}^B y_e^{\prime *b}, \tag{2}$$

where m^A and m^B are the transfer matrix from the IP to A $((x, x', y, y')_{\rm IP} \to (x, x', y, y')_A)$ and the transfer matrix from IP to the B $((x, x', y, y')_{\rm IP} \to (x, x', y, y')_B)$, respectively. The subscripts e and p represent the e^- and e^+ beams, respectively. The superscripts a and b correspond to after and before the collision. Asterisks denote the values at the IP and primes indicate angles. Using the transfer matrices, the vertical beam-beam kick that the e^- beam receives is written as

$$\Delta y_e^{\prime *} = y_e^{\prime *a} - y_e^{\prime *b} = \left(\frac{y_e^A}{m_{34}^A} - \frac{y_e^B}{m_{34}^B}\right) - \left(\frac{m_{33}^A}{m_{34}^A} - \frac{m_{33}^B}{m_{34}^B}\right) y_e^*. \tag{3}$$

Similarly, the e^+ beam receives the following vertical kick:

$$\Delta y_p^{\prime *} = y_p^{\prime *a} - y_p^{\prime *b} = \left(\frac{y_p^C}{m_{34}^C} - \frac{y_p^D}{m_{34}^D}\right) - \left(\frac{m_{33}^C}{m_{34}^C} - \frac{m_{33}^D}{m_{34}^D}\right) y_p^*. \tag{4}$$

From Eqs. (3) and (4), a new parameter $\Delta y_{\rm can}^{\prime *}$ called the "canonical vertical kick" is obtained as follows:

$$\Delta y'^{*}_{\rm can} \equiv \frac{\frac{y_e^A}{m_{34}^A} - \frac{y_e^B}{m_{34}^B}}{\frac{m_{33}^A}{m_{34}^A} - \frac{m_{33}^B}{m_{34}^B}} - \frac{\frac{y_p^C}{m_{34}^C} - \frac{y_p^D}{m_{34}^D}}{\frac{m_{33}^C}{m_{34}^C} - \frac{m_{33}^D}{m_{34}^D}} \tag{5}$$

$$= \frac{\Delta y'^{*}_{e}}{\frac{m_{33}^A}{m_{34}^A} - \frac{m_{33}^B}{m_{34}^B}} - \frac{\Delta y'^{*}_{p}}{\frac{m_{33}^C}{m_{34}^C} - \frac{m_{33}^D}{m_{34}^D}} + \Delta y^* \tag{6}$$

$$= -K_y \Delta y^*, \tag{7}$$

where

$$K_y = \frac{k_e}{m_e} + \frac{k_p}{m_p} - 1, \tag{8}$$

$$\Delta y'^{*}_{e} = -k_e \Delta y^*, \tag{9}$$

$$\Delta y'^{*}_{p} = k_p \Delta y^*, \tag{10}$$

$$m_e = \frac{m_{33}^A}{m_{34}^A} - \frac{m_{33}^B}{m_{34}^B}, \tag{11}$$

$$m_p = \frac{m_{33}^C}{m_{34}^C} - \frac{m_{33}^D}{m_{34}^D}, \tag{12}$$

and

$$\Delta y^* \equiv y_e^* - y_p^*. \tag{13}$$

In the expressions above, we treat only the linear part of the beam-beam force. The horizontal canonical kick can be expressed similarly. The canonical parameter is proportional to the vertical offset at the IP (Δy^*) and is therefore a good parameter to be used for collision feedback. The parameters m_e and m_p in Eq. (7) are constants calculated from the transfer matrices, while k_e and k_p are functions of beam-beam parameters and depend on the beam current and the beam sizes. Here, one should note that the canonical kick parameters are expressed in units of length. To make the physical meaning of this parameter clear, let us consider a simplified situation where the four BPMs are located an equal distance from the IP ($L_{\rm BPM}$) and there are no optical devices between the BPMs and the IP. In this situation, the vertical canonical beam-beam kick has a simple form as

$$\Delta y'^{*}_{\rm can} = -\left(\frac{L_{\rm BPM}}{2} k_e + \frac{L_{\rm BPM}}{2} k_p - 1\right)\Delta y^*. \tag{14}$$

In Eq. (14), the third term is usually negligibly small compared with the other terms. The other two terms denote (half of) orbit displacement due to the beam-beam kick. The canonical beam-beam kick parameters essentially express orbit changes detected at the positions of the BPMs due to the beam-beam kicks. One should also note that it is not possible to determine values of the beam-beam kick or those of the orbit offset at the IP from the beam-beam kick parameters. If one assumes the beam-beam parameter, one can estimate the value of the beam offset at the IP. This estimation is done in the following section. If one employs one more BPM for each beam, it is possible to determine the value of the beam-beam kick, since three unknown parameters, i.e. a beam position at the IP, an angle at the IP, and the beam-beam kick, can be determined by monitoring the beam orbit at three BPM positions. However, such an additional BPM has to be located in some distance from the two existing BPMs. This means that orbit measurements with this additional BPM are easily affected by the mechanical movement of the QCS magnets. We experienced that the orbit feedback by using such three BPMs does not work well maybe due to this problem. The QCS BPMs also suffer this effect slightly. However, the amount of the effect is within a tolerable range, since they are located very close to the QCS magnets.

The canonical crossing angle between the two beams can be also defined. The following equation gives the vertical canonical crossing angle $\theta_{y{\rm can}}$:

$$\theta_{y\,{\rm can}} \equiv \frac{\frac{y_e^A}{m_{33}^A} - \frac{y_e^B}{m_{33}^B}}{\frac{m_{34}^A}{m_{33}^A} - \frac{m_{34}^B}{m_{33}^B}} - \frac{\frac{y_p^C}{m_{33}^C} - \frac{y_p^D}{m_{33}^D}}{\frac{m_{34}^C}{m_{33}^C} - \frac{m_{34}^D}{m_{33}^D}}. \tag{15}$$

The idea of the orbit feedback is to maintain the optimum collision condition by keeping the canonical kicks and crossing angles at certain target values. In principle, the target values should be zero. However, we have to employ nonzero target values due to some offsets in the BPM readings. As is described below, we have to change the target values from time to time to maximize the luminosity.

C. Feedback algorithm

The feedback parameter for the nth iteration, y_n, can be expressed by a linear combination of the past N ($\equiv$ dimension) data points as

$$y_n = \sum_{k=1}^{N} c_k y_{n-k}. \tag{16}$$

The previous feedback quantities, y_{n-1}, y_{n-2}, etc., can be expressed similarly and the following M ($\equiv$ depth) sets of linear equations are obtained using a set of coefficients, c_k:

$$\begin{pmatrix} y_{n-1} & y_{n-2} & y_{n-3} & y_{n-4} & y_{n-5} & y_{n-6} \\ y_{n-2} & y_{n-3} & y_{n-4} & y_{n-5} & y_{n-6} & y_{n-7} \\ y_{n-3} & y_{n-4} & y_{n-5} & y_{n-6} & y_{n-7} & y_{n-8} \\ \vdots & \vdots & \vdots & \vdots & \vdots & \vdots \end{pmatrix} \begin{pmatrix} c_1 \\ c_2 \\ c_3 \\ c_4 \\ c_5 \\ c_6 \end{pmatrix} = \begin{pmatrix} y_n \\ y_{n-1} \\ y_{n-2} \\ \vdots \\ \vdots \\ \vdots \end{pmatrix}. \tag{17}$$

The coefficients c_k can be solved for as long as depth $\geq$ dimension. N and M are chosen empirically to be 6 and 48, respectively, for the current operation. Using c_k, the next feedback parameter y^*_{n+1} is predicted. Here, one should carefully distinguish this value (y^*_{n+1}) from the actually measured value (y_{n+1}) at the next step. The feedback action is done by making an orbit bump corresponding to the following quantity:

$$\Delta y = -G y^*_{n+1}. \tag{18}$$

Here, G is a gain factor which is determined empirically. In the actual operation, as the feedback parameter, we take the difference of $\Delta y'^*_{\text{can}}$ or $\theta_{y\text{can}}$ from their target values. Prior to applying this algorithm to the actual feedback routine, a computer simulation was done to confirm its effectiveness [7].

III. SYSTEM PERFORMANCE

The goal of this section is to give an estimate of system performance. Even with the orbit feedback, there still remains small orbit fluctuation. We first give a typical amplitude of fluctuation and then estimate how much degradation in the luminosity is brought by orbit fluctuation.

A. Machine parameters

Machine parameters related to the feedback system are summarized in Table I. These parameters are typical of the machine operation in the spring of 2004. Most of the performance data shown in this section were taken in this period.

B. System performance

At present, we only use the QCS BPMs. A comparison between QCS BPMs and OctoPos BPMs is given in the next section. To evaluate the feedback performance, we investigated fluctuations of feedback parameters described in the previous section. Figure 2 shows the fluctuation of the canonical vertical kick ($\Delta y'^*_{\text{can}}$). During the period shown in Fig. 2, the machine condition was stable and no parameter scan, which we frequently make for searching better parameters, was done. The orbit feedback for the vertical offset and the vertical crossing angle was on. The canonical vertical kick fluctuates around the target value. In this case, the target value was -1.625 mm, which had been determined by a scan to maximize the luminosity. Figure 3 shows a histogram of the deviations of the canonical vertical kick from the target value with the same data as Fig. 2. One standard deviation of this distribution is about 0.035 mm.

The next task is to estimate how much a degradation of the luminosity this fluctuation corresponds to. For this purpose, we can employ a target scan of the vertical offset. An example of such a scan is shown in Fig. 4. This scan was done on the same day as the data in Fig. 2. In this figure, a fitted curve using a quadratic function is also shown. By using this curve, we found that the rms value of the 0.035 mm of the data in Figs. 2 and 3 corresponded to a luminosity degradation of about 0.65%.

TABLE I. Machine parameters of KEKB related to the orbit feedback system.

	LER	HER	
Beam energy	3.5	8.0	GeV
Circumference	3016		m
I_{beam}	1650	1220	mA
Number of bunches	1294		
I_{bunch}	1.28	0.94	mA
Averaged bunch spacing	2.35		m
Horizontal emittance	18	24	nm
β^*_x/β^*_y	59/5.2	56/6.5	cm/mm
Vertical beam size at IP	2.1	2.1	μm
ν_x/ν_y	0.505/0.535	0.513/0.582	
ξ_x/ξ_y	0.113/0.074	0.072/0.057	
Peak luminosity	1.4		$10^{34}/\text{cm}^2/\text{sec}$

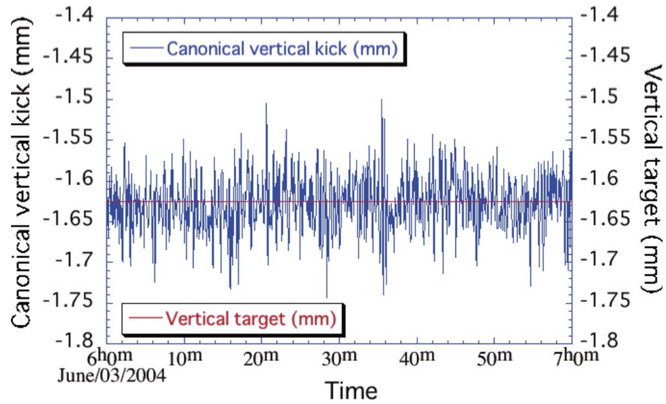

FIG. 2. (Color) Fluctuation of the canonical vertical kick ($\Delta y'^*_{\text{can}}$). The target value is also shown.

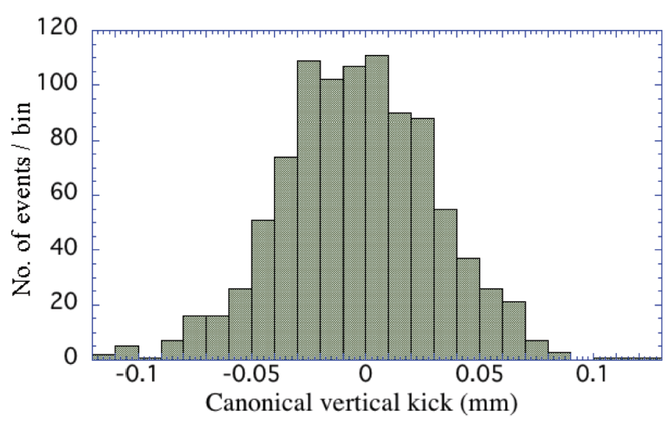

FIG. 3. (Color) Histogram of the canonical vertical kick. The data is the same as that in Fig. 2. The target value is subtracted so that the center of the distribution is at zero.

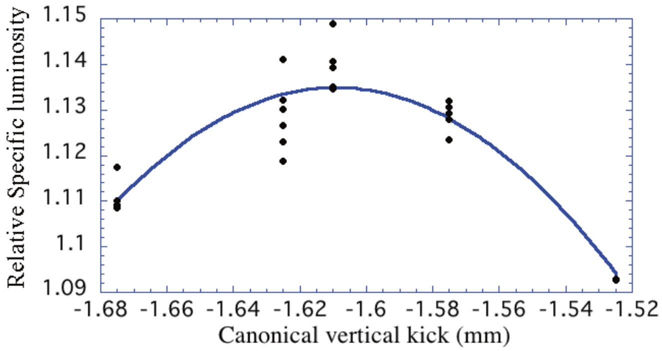

FIG. 4. (Color) Typical result of the target scan of the vertical offset. A fitted curve using a quadratic function is also shown.

To discuss system performance in more detail, it is needed to translate the fluctuation of the canonical vertical kick in Fig. 2 to the real vertical offset. For this purpose, we have to estimate the value of K_y in Eq. (8). The values of k_e and k_p in (9) and (10) can be estimated by using ξ_y and β_y^* in Table I. Here, we assumed the coherent beam-beam tune shift to be half of the incoherent beam-beam tune shift (the beam-beam parameter) with an assumption of the rigid Gaussian approximation. By using k_e and k_p thus estimated together with m_e and m_p in (11) and (12), we estimated K_y to be about 483. With this value, we found that 0.035 mm (the rms value of the canonical vertical kick) corresponds to about 0.07 μm of the vertical offset at the IP. This value is significantly small compared with the vertical beam size of about 2.1 μm shown in Table I.

It is useful to compare the luminosity degradation obtained from the scan with that of a beam-beam simulation, since the degradation with such a small offset cannot be explained by the geometrical loss. Figure 5 shows a comparison of the experimental data of the luminosity degradation due to the vertical offset with that of the beam-beam simulation. The beam-beam simulation was done by using a strong-strong simulation code developed at KEK [14].

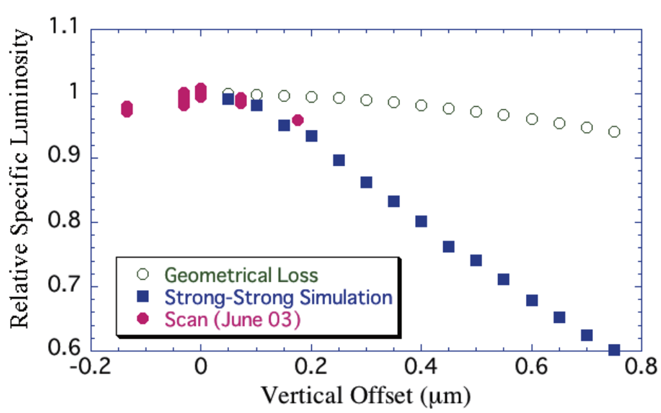

FIG. 5. (Color) Luminosity degradation due to the vertical offset. Both an experimental result and a strong-strong simulation are shown. Also shown is a calculation of a geometrical loss.

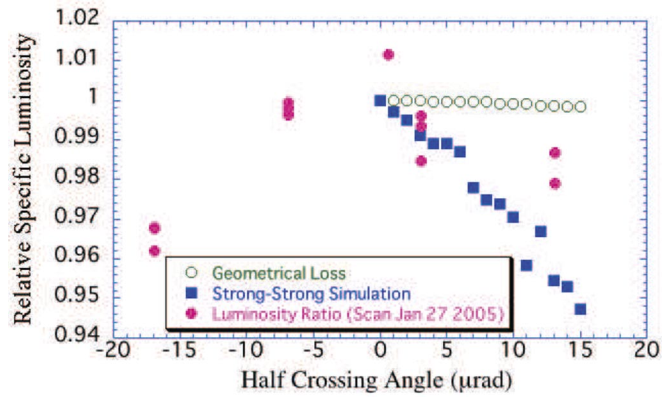

FIG. 6. (Color) Luminosity degradation due to the vertical crossing angle. Both an experimental result and a strong-strong simulation are shown. Also shown is a calculation of a geometrical loss.

The figure shows that the luminosity degradation in the experiment is much larger than the geometrical loss and can be well reproduced by the simulation. To sum up, although the luminosity reduction due to the vertical offset is much larger than the geometrical loss, our orbit feedback system works well to minimize the loss.

We evaluated the performance for the vertical crossing angle with a similar method. Here, we summarize only the result. The rms value of the fluctuation of the vertical canonical crossing angle defined by Eq. (15) for 1 hour on January 26, 2005 is about 0.0070 mrad which corresponds to a half crossing angle of 3.5 μrad. From a target scan for the vertical crossing angle, the luminosity reduction due to this fluctuation is estimated to be about 0.56%. This luminosity loss seems reasonably small. Figure 6 shows a comparison of the experimental data of the luminosity degradation due to the vertical crossing angle with that of the beam-beam simulation. The figure shows that the luminosity degradation in the experiment is much larger than the geometrical loss. Although the agreement between the experiment and the simulation is not as good as in the case of the vertical offset, it seems to be still within a tolerable range.

IV. OPERATIONAL EXPERIENCE

We have been using the orbit feedback system for more than 6 years. We have accumulated much experience with the system. In this section, we describe some details of our experience. We mention five topics in this section. The first two topics are connected to the system design. We describe our experience on how large and how fast the orbit fluctuations are in the KEKB rings. The third topic is the stability of the feedback target values. A weak point of our feedback system based on the measurement of the beam orbits around the IP is that the target values change as a function of time. We mention lots of efforts which have been made for solving this problem. The fourth topic is a comparison between the feedback using the OctoPos BPMs and that using the QCS BPMs. In the original plan, we planned to utilize the OctoPos BPMs for the feedback. However, we found that the system using the QCS BPMs is superior. We explain the reason for this. In the last topic, we briefly describe an orbit feedback in the horizontal direction.

A. How seriously do we need the feedback?

In the design phase of KEKB, we have almost no idea on how seriously we need the orbit feedback system. Through experience in operating KEKB, we recognized that the beam orbits largely change as a function of the beam currents. The mechanism of the orbit drifts depending on the beam currents seems to be movements of quadrupole magnets. Heating of vacuum chambers due to synchrotron lights seems to be responsible for the movements. Actually, we observe large movements of the IR magnets dependent on the beam currents. We have a global orbit correction system called continuous closed orbit correction (CCC) to compensate for the orbit drifts [6]. The system works continuously during the beam operation with a cycle of about 20 seconds. The CCC system corrects orbit drifts due to other mechanisms such as temperature variations of the KEKB tunnel. However, it turned out that we need the orbit feedback system around the IP even with CCC to keep the luminosity.

Figure 7 shows a typical behavior of the orbit feedback system. In the figure, plotted is the history of the vertical bump amplitude at the IP created by the orbit feedback system for two hours. During this period, the machine condition was very stable and the luminosity was kept almost constant owing to the orbit feedback system. The beam currents were also kept almost constant thanks to the continuous beam injection mode [15]. The period was not a special one but was chosen rather randomly on the condition that the machine status is stable. The change of the vertical offset during this period is much larger than the range in Fig. 5 or even larger than the vertical beam size. This means that the vertical offset at the IP would largely change for a short time without the feedback. The amount of the offset change is unexpectedly large. Some part of the offset change may be created by the CCC system. Therefore, the orbit feedback system is vital for KEKB.

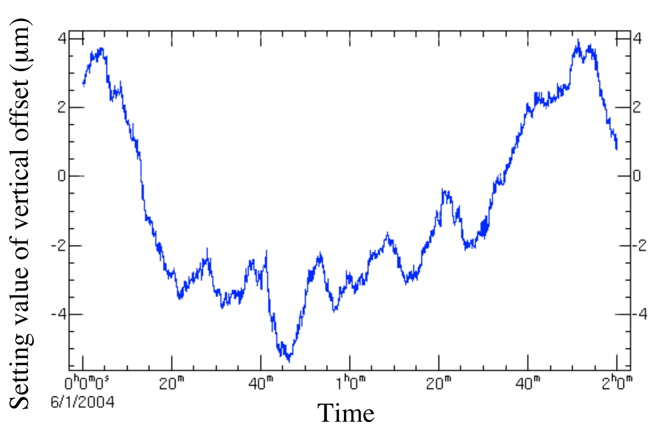

FIG. 7. (Color) History of the vertical bump amplitude at the IP.

B. How fast feedback do we need?

The cycle of the present feedback system is about 4 seconds, which is mainly determined by the speed of the orbit measurement. We need to investigate whether this speed of the feedback is sufficient or not to compensate the orbit drift. In 2000, we tried to measure faster orbit drifts. This was done by decreasing the averaging time of the measurements with the same BPM system as is utilized for the orbit measurement in the rings. In this mode, the position resolution of the measurement is estimated to be around 12 μm. A Fourier spectrum of the orbit change up to 50 Hz was obtained. In this measurement, we found a peak at around 13 Hz in both rings. This orbit oscillation makes a vertical angle rather than the offset. A typical amount of the vertical angle at the IP was about 20 μrad in LER. The cause of this orbit oscillation seems to be the mechanical vibration of the QCS magnets. As is shown in Fig. 3, a half crossing angle of 10 μrad brings a luminosity loss of about 3%. However, the orbit changes of the two beams make the relative crossing angle smaller and the luminosity loss may decrease down to about 1%. Except for this oscillation at around 13 Hz, no significant fast oscillation was observed. Therefore, the present cycle of 4 seconds seems to be enough except for the small loss in the luminosity due to the 13 Hz oscillation.

C. Stability of the target values

The orbit feedback system is successfully employed at KEKB for minimizing the luminosity degradation due to the vertical orbit drifts. A remaining problem with the system is that the optimum value of the feedback target changes as time goes by. To trace their changes, we rather frequently (typically once an 8-hour shift) need to do the target scan for optimum values. It takes about 20 min for one scan. During the scan, the averaged luminosity slightly decreases by typically about 1%. Assuming that we scan the targets of the vertical offset and the vertical crossing angle once per 8-hour shift, the luminosity loss due to the scans is about 0.04% for each parameter. This value is more than one order of magnitude smaller than the loss due to the fluctuations of these parameters. When the machine condition is stable, in each scan, we usually find that the degradation of the luminosity due to the drift of the optimum target values is well below 1%. Therefore, in case of a stable machine condition, we estimate that the luminosity loss due to the drift of the optimum values for the feedback target values is much less than 1% for each parameter.

A problem was that the optimum target value of the offset changes largely after beam aborts. We have made many efforts to solve this problem. Although the cause of the target change has not been understood completely, the most possible candidate is mechanical movement of the BPMs or the QCS magnets. Unlike the other BPMs, the QCS BPMs are not rigidly fixed to the quadrupole magnets and they can easily move according to movement of the vacuum chambers. Our observations have shown that heating of vacuum chambers brings sizable mechanical movement of the vacuum chamber and of the quadrupole magnets. In the summer shutdown in 2003, we extensively reinforced the cooling power of the IR vacuum chambers. After this, the drift of the target values was alleviated to some extent, although the drift did not disappear completely. Also, we introduced displacement monitors which watch the mechanical shifts of the BPMs (A, B, C, and D) in Fig. 1. Since the introduction of the monitors, the measured data of the beam positions at the BPMs have been corrected with information on the mechanical drifts. From the beginning of 2004, we started the beam operation with the continuous injection scheme [15]. With this scheme, the beam currents are almost kept constant except after beam aborts. In addition to these efforts, we started making correction for the movements of the QCS magnets in May 2006. Since the BPMs (A, B, C, and D) in Fig. 1 are located on the arc sides of the QCS magnets, the measured values of the vertical offset and the crossing angle are affected by the movements of these magnets. Prior to this correction, we introduced gap sensors to measure the mechanical positions of these magnets. As a result of these efforts, the changes of the optimum target values after beam aborts have been reduced to almost negligible levels.

Even with these efforts, however, there still remain some slow drifts of the target values. A history of the change of the target values for one month after these efforts is shown in Fig. 8. This indicates that there are some unknown sources which bring the target changes. We need more study in this regard. However, even with the slow drift of the target values, the luminosity loss due to the change of the optimum target values is well below 1%.

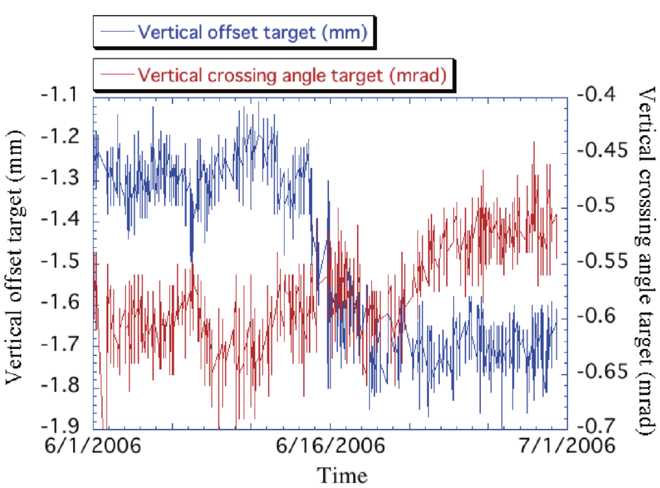

FIG. 8. (Color) History of change of the feedback target values.

D. Comparison between OctoPos BPMs and QCS BPMs

An evaluation and comparison of feedback performance between the two different sets of BPMs (OctoPos BPMs and QCS BPMs) was carried out in 2002. The canonical vertical kick, which is the input to the feedback system, was switched from the QCS BPMs to the OctoPos BPMs at the beginning of one shift and kept in use for the next 8 hours. The canonical kick monitored by the OctoPos BPMs is plotted in Fig. 9 along with the target value. As is seen from this plot, the optimum target value was not constant through a beam fill but has a strong dependence on the beam currents. Also shown in Fig. 9 are the HER and LER beam currents. This strong beam current dependence is somewhat troublesome as the operators have to chase the target value all the time. The beam-beam kick calculated using the QCS BPM data does not show such beam current dependence.

Using the data in Fig. 9, the feedback performance was evaluated. Figure 10 shows a comparison between different BPM systems. The target value is subtracted from the monitored value. The canonical vertical kick was converted to the vertical offset between the two beams at the IP in those plots using the value of K_y mentioned in Sec. III. Both have a Gaussian distribution around zero (the target values) with a standard deviation of $\sim 0.1\ \mu$m. The feedback with the QCS BPMs gives a narrower distribution. However, the difference may not be significant as the QCS BPMs had been used a long time and the feedback parameters, such as the feedback gain, may have been more finely tuned than the feedback with the OctoPos BPMs. Although both BPM systems gave satisfactory performance, the QCS BPMs are currently used as the monitor of the canonical vertical kick. This is because the OctoPos system has a strong dependence on the beam currents and the need for optimizing the target value during the fill is operationally difficult. After introducing the continuous injection scheme [15] at the beginning of

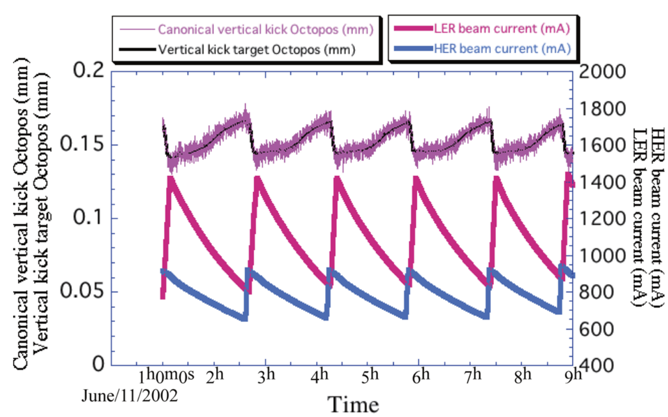

FIG. 9. (Color) Canonical vertical kick monitored by the OctoPos BPMs together with the feedback target value. The HER and LER beam currents are also shown.

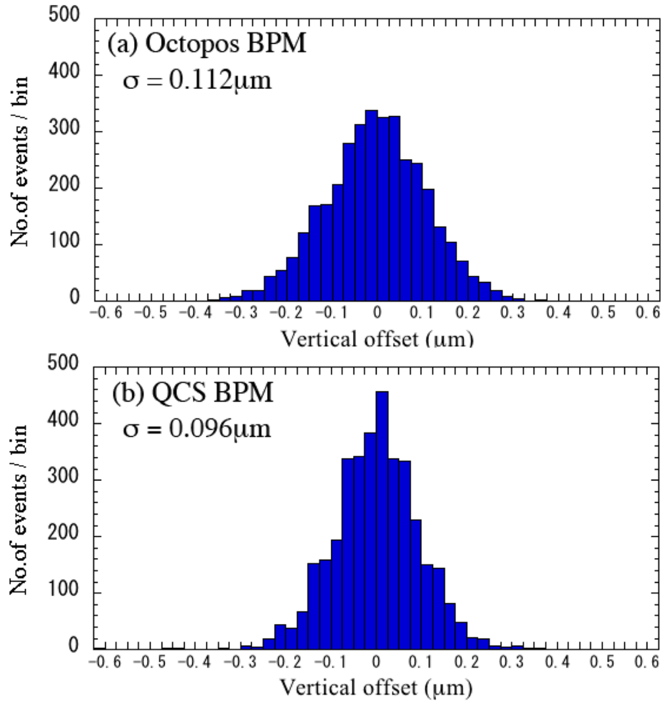

FIG. 10. (Color) The comparison between the feedback with the OctoPos BPMs (a) and the QCS BPMs (b). The abscissa is translated to the vertical offset of the two beams at the IP. The QCS system shows a slightly narrower distribution.

2004, the operational beam currents are kept almost constant and the current dependence of the OctoPos BPMs became less serious. However, we are still using the QCS BPMs for the feedback, since the beam current dependence still makes the beam operation difficult during the transitional period after beam aborts.

E. Horizontal feedback

In the horizontal direction, we do not utilize the orbit feedback based on the beam-beam deflection described in this paper. We had been bothered by somewhat strange phenomena on the horizontal offset. Key points of the observations on the behavior of the beams to the horizontal offset are in the following. (i) A zero offset does not give the maximum luminosity. Instead, at some optimum nonzero value of the offset (typically ~50 μm), the luminosity becomes maximum. (ii) The vertical beam size of LER is very sensitive to the horizontal offset and is not symmetric with respect to the sign of the offset.

More detailed descriptions of the phenomena have been given elsewhere [16,17]. This asymmetry in the vertical beam size has been utilized to control the horizontal offset, as it has even better sensitivity than the horizontal beam-beam deflection [18]. This feedback monitors the LER vertical beam size. The goal of the feedback is to keep the beam size at a target value which depends on the beam current and is determined empirically. Empirically, we know that the LER beam size shrinks with a horizontal offset change in the positive direction, which means that the HER beam is on the outer side of the ring at the IP, and enlarges with an offset change in the negative direction. By controlling the horizontal offset properly, we can keep the beam size (and the luminosity) at an optimum condition. Although the algorithm is simple, this feedback has been successfully working at KEKB.

V. DISCUSSION

In this section, we discuss two subjects. In the first subject, we reconsider the system design by estimating resolution of critical parameters of the feedback system. In the second, we give a comparison between the deflection-driven and the luminosity-driven feedback systems.

A. Resolution of feedback parameters

Resolution of the orbit measurements is about 2 μm with beam currents in the usual physics run. With this resolution, we can estimate resolution of the feedback parameters, $y'^*_{\rm can}$ and $\theta_{y\rm can}$. By using Eqs. (5), (7), and (15), we get 8.9 μm and 1.3 μrad for resolution of $y'^*_{\rm can}$ and $\theta_{y\rm can}$, respectively. Here, we took the propagation of errors into account with the assumption that there are no correlations between errors in the orbit measurements. Resolution for $y'^*_{\rm can}$ of 8.9 μm corresponds to 0.018 μm of the vertical offset at the IP (Δy^*), if we use the value of K_y in Sec. III. This resolution is reasonably small considering the vertical-offset dependence of the luminosity shown in Fig. 5. Resolution for $\theta_{y\rm can}$ is also small enough considering the crossing-angle dependence of the luminosity shown in Fig. 6. Also in comparison with the fluctuations of the monitor values for the vertical offset and the crossing angle, resolution above is by a factor 4 or 5 smaller.

As for the setting errors of the bump orbits, we have to consider the quantization error due to the use of DAC. The dynamic ranges of the vertical offset and angle settings are about ± 180 μm and ± 300 μrad, respectively. Since the steering magnets are controlled by using a DAC with ± 2048 steps, the minimum steps of the offset and the angle are about 0.09 μm and 0.15 μrad, respectively. The quantization error of the vertical angle is almost one order smaller than its fluctuation and seems small enough. However, that of the vertical offset is marginal, since its value is comparable to (or even slightly larger than) the fluctuation of the vertical offset. It seems that this quantization error is one of the major sources of its fluctuation. Therefore, there remains some small room for improvement in this regard. In the design of the orbit feedback system, we primarily considered the geometrical loss of the luminosity. However, this was obviously insufficient, since the luminosity loss due to the beam-beam blowup is much more severe. Fortunately, the system performance seems still excellent owing to margins of the system design.

B. Comparison between the deflection-driven and the luminosity-driven feedback systems

At KEKB, the deflection-driven feedback has been utilized for the vertical offset. Its sensitivity seems excellent and the luminosity loss due to the fluctuation of the vertical offset is suppressed less than 1% using this system as described in Sec. IV. As for the vertical crossing angle, a similar method which measures the beam orbits around IP has been utilized and the luminosity loss can be suppressed also less than 1%. One problem with this kind of system is that the target values of the feedback system drift, for several reasons. Lots of efforts have been devoted to suppress these drifts. As a result of the efforts, the luminosity loss due to the drifts of the target values has been successfully suppressed much less than 1%, although we need to do the target scan typically once per 8-hour shift to trace the slow drifts. Experience at KEKB has proven that the deflection-driven feedback works excellently at a current double-ring collider.

On the other hand, at PEP-II, the luminosity-driven feedback has been successfully utilized for years [8,9]. The deflection-driven feedback was replaced by this at the very beginning of the history due to the reliability problem. Although the reliability has been a problem also at KEKB, the problem has not been so serious and was almost solved. Experience at PEP-II has proven that the luminosity-driven approach also works very well at a current double-ring collider. A possible problem with the luminosity-driven system is that some loss in the luminosity is unavoidable due to an intentional change of the beam orbits which is needed to search for the optimum collision conditions. However, no concrete value on this loss is found in literature. Therefore, we cannot make a comparison on the ultimate performance between the deflection-driven feedback and the luminosity-driven feedback.

In future double-ring colliders or linear colliders, the possibility to incorporate both systems should be pursued, since the two systems seem very complementary. For example, by working one of the feedback system and monitoring input parameters for the other, one may be able to obtain information to improve the performance of both systems. In addition, in some situation, one of the two systems becomes preferable. For example, at KEKB, the fast luminosity monitor has a problem of narrow acceptance and the luminosity-driven feedback does not work well. At PEP-II, the deflection-driven feedback does not work well due to the reliability problem. With such a unified system, one can switch the two feedback systems according to the situation.

VI. CONCLUSIONS

In double-ring colliders such as KEKB, an orbit feedback system for maintaining the beam orbits around the IP is vital. Without such a system, we cannot maintain the luminosity even for a short period. At KEKB, the most important source of the orbit drift is movement of the IR quadrupole magnets. The effect of the global orbit correction system (CCC) also seems to be a source of the orbit drifts around the IP. At KEKB, the orbit feedback system in the vertical direction monitors the beam orbits of both beams at the final focus quadrupole magnets. The vertical beam offset at the IP is detected by using the beam-beam deflection method and the crossing angle is obtained by simply measuring the beam positions. This system has been working very well and suppresses the luminosity loss due to the vertical orbit drift to below 1%. A problem with this system has been the drift of the target values for the feedback. As a result of lots of efforts, however, this problem was almost solved. Experience at KEKB has shown that the scheme based on the orbit measurements around the IP is expected to be applicable to the orbit feedback system around the IP in future double-ring colliders or linear colliders.

ACKNOWLEDGMENTS

The authors would like to express their thanks to the KEKB operator group from Mitsubishi Electric System and Service. The operators' experience of the beam operation by using the orbit feedback system has been greatly helpful for upgrading the system. The authors also thank the members of the KEKB commissioning group for their useful comments and discussion on the feedback system.

[1] KEKB B-Factory Design Report, KEK Report No. 95-7, 1995.

[2] P. Bambade, R. Erickson, W. A. Koska, W. Kozanecki, N. Phinney, and S. R. Wagner, Phys. Rev. Lett. **62**, 2949 (1989).

[3] F. Rouse, T. Gromme, W. Kozanecki, and N. Phinney, Proceedings of Particle Accelerator Conference, San Francisco, CA, 1991.

[4] Y. Funakoshi, M. Tejima, and H. Ishii, in *Proceedings of the Particle Accelerator Conference, Dallas, TX, 1995* (IEEE, Piscataway, 1995).

[5] C. Bovet, M. Hildreth, M. Lamont, H. Schmickler, and J. Wenninger in Proceedings of the 5th European Particle Accelerator Conference, Sitges Barcelona, Spain, 1996.

[6] K. Akai, N. Akasaka, A. Enomoto, J. Flanagan, H. Fukuma, Y. Funakoshi, K. Furukawa, T. Furuya, J. Haba, S. Hiramatsu, K. Hosoyama, T. Ieiri, N. Iida, H. Ikeda, S. Kamada, T. Kamitani, S. Kato, M. Kikuchi, E. Kikutani, H. Koiso, S. Kurokawa, M. Masuzawa, T. Matsumoto, T. Mimashi, T. Mitsumashi, T. T. Nakamura, Y. Ogawa, K. Ohmi, Y. Ohnishi, S. Ohsawa, N. Ohuchi, K. Oide, E. Perevedentsev, K. Satoh, M. Suetake, Y. Suetsugu, T. Suwada, M. Tawada, M. Tejima, M. Tobiyama, S. Uno, Y. Wu, N. Yamamoto, M. Yoshida, M. Yoshioka, S. Yoshimoto, and F. Zimmermann, Nucl. Instrum. Methods Phys. Res., Sect. A **499**, 191 (2003).

[7] M. Masuzawa, J. W. Flanagan, Y. Funakoshi, and K. Oide, in *Proceedings of the 7th European Particle Accelerator Conference, Vienna, Austria, 2000* (EPS, Geneva, 2000).

[8] W. Kozanecki, Y. Cai, S. Ecklund, C. Field, A. S. Fisher, L. Hendrickson, T. Himel, M. Minty, M. Placidi, J. T. Seeman, M. Sullivan, U. Wienands, and M. S. Zisman, in Proceedings of the ICFA Workshop on e^+e^- Factories, 1999 (Factories 1999), Tsukuba, Japan.

[9] L. Hendrickson, T. Gromme, P. Grossberg, T. Himel, D. Macnair, R. Sass, H. Smith, N. Spencer, M. Sullivan, U. Wienands, and L. Yasukawa, in *Proceedings of the 7th European Particle Accelerator Conference, Vienna, Austria, 2000* (EPS, Geneva, 2000).

[10] M. Tejima, S. Hiramatsu, M. Masuzawa, K. Oide, K. Satoh, and M. Tobiyama, *Proceedings of the 8th European Particle Accelerator Conference, Paris, France, 2002* (EPS, Geneva, 2002).

[11] M. Arinaga, J. Flanagan, S. Hiramatsu, T. Ieiri, H. Ikeda, H. Ishii, E. Kikutani, T. Mimashi, T. Mitsumashi, H. Mizuno, K. Mori, M. Tejima, and M. Tobiyama, Nucl. Instrum. Methods Phys. Res., Sect. A **499**, 100 (2003).

[12] N. Akasaka, A. Akiyama, S. Araki, K. Furukawa, T. Katoh, T. Kawamoto, I. Komada, K. Kudo, T. Naito, T. Nakamura, J. Odagiri, Y. Ohnishi, M. Sato, M. Suetake, S. Takeda, Y. Takeuchi, N. Yamamoto, M. Yoshioka, Nucl. Instrum. Methods Phys. Res., Sect. A **499**, 138 (2003).

[13] http://acc-physics.kek.jp/SAD/sad.html.

[14] K. Ohmi, Phys. Rev. E **62**, 7287 (2000).

[15] S. Uno *et al.* (to be published).

[16] Y. Funakoshi, in Proceedings of the ICFA Workshop on e^+e^- Factories, 2001 (Factories 2001), Ithaca, New York.

[17] T. Ieiri, Y. Funakoshi, T. Kawamoto, M. Masuzawa, M. Tawada, M. Tombiyama, and S. S. Win, in *Proceedings of the 9th European Particle Accelerator Conference, Lucerne, Switzerland, 2004* (EPS, Geneva, 2004).

[18] M. Tanaka, Y. Sato, S. Iida, T. Kitabayashi, T. Kawasumi, K. Yoshii, T. Aoyama, S. Shimomura, K. Sugita, T. Nakamura, T. Ohkubo, S. Fuke, Y. Funakoshi, H. Koiso, N. Iida, M. Masuzawa, and K. Oide, in Proceedings of the 14th Symposium on Accelerator Science and Technology, Tsukuba, Japan, 2003, http://conference.kek.jp/sast03/, in Japanese.